SLAC-PUB-8830
*BABAR*-PROC-01/11
hep-ex/0105019
10 May, 2001

# Charmless Hadronic $B$ Decays at *BABAR*

Thomas Schietinger

Stanford Linear Accelerator Center, Stanford, CA 94309
E-mail: Thomas.Schietinger@SLAC.Stanford.edu

(for the *BABAR* Collaboration)

**Abstract**

We present several searches for charmless hadronic two-body and three-body decays of $B$ mesons from electron-positron annihilation data collected by the *BABAR* detector near the $\Upsilon(4S)$ resonance. We report the preliminary branching fractions $\mathcal{B}(B^0 \to \pi^+\pi^-) = (4.1 \pm 1.0 \pm 0.7) \times 10^{-6}$, $\mathcal{B}(B^0 \to K^+\pi^-) = (16.7 \pm 1.6 \pm 1.3) \times 10^{-6}$, $\mathcal{B}(B^0 \to \rho^\mp\pi^\pm) = (49 \pm 13^{+6}_{-5}) \times 10^{-6}$, $\mathcal{B}(B^+ \to \eta' K^+) = (62 \pm 18 \pm 8) \times 10^{-6}$, and present upper limits for nine other decays.

Contributed to the Proceedings of the
Lake Louise Winter Institute on Fundamental Interactions,
18–24 February 2001, Lake Louise, Alberta, Canada

*Stanford Linear Accelerator Center, Stanford University, Stanford, CA 94309*

Work supported in part by Department of Energy contract DE-AC03-76SF00515.

# 1 Introduction

The study of $B$ meson decays into charmless hadronic final states plays an important role in the understanding of CP violation. In the Standard Model, all CP-violating phenomena are a consequence of a single complex phase in the Cabibbo-Kobayashi-Maskawa (CKM) quark-mixing matrix [1]. The Belle and *BABAR* collaborations have presented results [2, 3] on measurements of CP-violating asymmetries in $B$ decays into final states containing charmonium, leading to constraints on the angle $\beta$ of the CKM unitarity triangle. Measurements of the rates and CP asymmetries for $B$ decays into the charmless final states $\pi\pi$ and $K\pi$ can be used to constrain the angles $\alpha$ and $\gamma$ of the unitarity triangle [4].

# 2 Detector and data

Here we present new measurements of the branching fractions for charmless hadronic decays of $B$ mesons in the final states[1] $\pi^+\pi^-$ and $K^+\pi^-$, and an upper limit for $B \to K^+K^-$, which are based on a data sample consisting of an integrated luminosity of 20.6 fb$^{-1}$ taken near the $\Upsilon(4S)$ resonance ("on-resonance"), corresponding to $(22.57 \pm 0.36) \times 10^6$ $B\overline{B}$ pairs. A data sample of 2.61 fb$^{-1}$ taken at a center-of-mass (CM) energy 40 MeV below the $\Upsilon(4S)$ resonance ("off-resonance") is used for continuum background studies.

We also report measurements of branching fractions and upper limits for $B$ decays into non-resonant three-body modes and modes containing $K^*$, $\rho$, $\omega$, and $\eta'$ resonances, which are based on a smaller data sample (see Sec. 4).

The data were collected with the *BABAR* detector at the PEP-II $e^+e^-$ collider at the Stanford Linear Accelerator Center. The collider is operated with asymmetric beam energies, producing a boost ($\beta\gamma = 0.56$) of the $\Upsilon(4S)$ along the collision axis ($z$). For the analyses described in this Letter, the most significant effect of the boost relative to symmetric collider experiments is to increase the momentum range of the two-body $B$ decay products from a narrow distribution centered at approximately 2.6 GeV/$c$ to a broad, approximately flat distribution extending from 1.7 to 4.2 GeV/$c$.

At this conference, the *BABAR* detector has been described in detail by Jim Panetta [5]. Here we only reemphasize that the identification of tracks as pions or kaons is based on the Cherenkov angle $\theta_c$ measured by a unique, internally reflecting Cherenkov ring imaging detector (DIRC). The $K$–$\pi$ separation varies as a function of momentum and is better than 8 standard deviations ($\sigma$) at 1.7 GeV/$c$ and decreases to $2.5\sigma$ at 4 GeV/$c$.

# 3 Analysis of $B^0 \to \pi^+\pi^-, K^+\pi^-, K^+K^-$

The selection of hadronic events for this analysis is based on track multiplicity and event topology. To reduce background from non-hadronic events, the ratio of Fox-Wolfram moments [6] $H_2/H_0$ is required to be less than 0.95 and the sphericity [7] of the event is required to be greater than 0.01.

All tracks are required to have a polar angle within the tracking fiducial region $0.41 < \theta < 2.54$ rad and a $\theta_c$ measurement from the DIRC. The latter requirement is satisfied by 91% of the tracks in the described fiducial region. We require a minimum number of Cherenkov photons associated with each $\theta_c$ measurement in order to improve the resolution. The efficiency of this requirement is

[1] Charge conjugate states are assumed throughout, except where explicitly noted.

97% per track. Tracks with a $\theta_c$ within $3\sigma$ of the expected value for a proton are rejected. Electrons are rejected based on specific ionization ($dE/dx$) in the DCH system, shower shape in the EMC, and the ratio of shower energy to track momentum.

The kinematic constraints provided by the $\Upsilon(4S)$ initial state and relatively precise knowledge of the beam energies are exploited to efficiently identify $B$ candidates. We define a beam-energy substituted mass $m_{\rm ES} = \sqrt{E_{\rm b}^2 - \mathbf{p}_B^2}$, where $E_{\rm b} = (s/2 + \mathbf{p}_i \cdot \mathbf{p}_B)/E_i$, and $\sqrt{s}$ and $E_i$ are the total energies of the $e^+e^-$ system in the CM and lab frames, respectively, and $\mathbf{p}_i$ and $\mathbf{p}_B$ are the momentum vectors in the lab frame of the $e^+e^-$ system and the $B$ candidate, respectively. The $m_{\rm ES}$ resolution is dominated by the beam energy spread and is approximately 2.5 MeV/$c^2$. Candidates are selected in the range $5.2 < m_{\rm ES} < 5.3$ GeV/$c^2$.

We define an additional kinematic parameter $\Delta E$ as the difference between the energy of the $B$ candidate and half the energy of the $e^+e^-$ system, computed in the CM system, where the pion mass is assumed for all charged $B$ decay products. The $\Delta E$ distribution is peaked near zero for modes with no charged kaons and shifted on average $-45$ MeV ($-91$ MeV) for modes with one (two) kaons, where the exact separation depends on the laboratory kaon momentum. The resolution on $\Delta E$ is about 26 MeV. Candidates with $|\Delta E| < 0.15$ GeV are accepted.

Detailed Monte Carlo simulation, off-resonance data, and events in on-resonance $m_{\rm ES}$ and $\Delta E$ sideband regions are used to study backgrounds. The contribution due to other $B$-meson decays, both from $b \to c$ and charmless decays, is found to be negligible. The largest source of background is from random combinations of tracks and neutrals produced in the $e^+e^- \to q\bar{q}$ continuum (where $q = u$, $d$, $s$ or $c$). In the CM frame this background typically exhibits a two-jet structure that can produce two high momentum, nearly back-to-back particles. In contrast, the low momentum and pseudoscalar nature of $B$ mesons in the decay $\Upsilon(4S) \to B\overline{B}$ leads to a more spherically symmetric event. We exploit this topology difference by making use of two event-shape quantities. The variable we considered that has the greatest discriminating power is the angle $\theta_S$ between the sphericity axes evaluated in the CM frame, of the $B$ candidate and the remaining tracks and photons in the event. The distribution of the absolute value of $\cos\theta_S$ is strongly peaked near 1 for continuum events and is approximately uniform for $B\overline{B}$ events. We require $|\cos\theta_S| < 0.9$, which rejects 66% of the background that remains at this stage of the analysis.

The second quantity used in the analysis is a linear combination of the nine scalar sums of the momenta of all tracks and photons (excluding the $B$ candidate decay products) flowing into $10^\circ$ polar angle intervals coaxial around the thrust axis of the $B$ candidate, in the CM frame (Fisher discriminant [8] $\mathcal{F}$). Monte Carlo samples are used to obtain the values of the coefficients, which are chosen to maximize the statistical separation between signal and background events. No restrictions are placed on $\mathcal{F}$. Instead, it is used as an input variable in a maximum likelihood fit, described below.

Signal yields are determined from an unbinned maximum likelihood fit that uses the following quantities: $m_{\rm ES}$, $\Delta E$, $\mathcal{F}$, and $\theta_c$. The likelihood for a given candidate $j$ is obtained by summing the product of event yield $n_k$ and probability $\mathcal{P}_k$ over all possible signal and background hypotheses $k$. The $n_k$ are determined by maximizing the extended likelihood function $\mathcal{L}$:

$$\mathcal{L} = \exp\left(-\sum_{k=1}^{M} n_k\right) \prod_{j=1}^{N} \left[\sum_{k=1}^{M} n_k \mathcal{P}_k\left(\vec{x}_j; \vec{\alpha}_k\right)\right] . \tag{1}$$

The probabilities $\mathcal{P}_k(\vec{x}_j; \vec{\alpha}_k)$ are evaluated as the product of probability density functions (PDFs) for each of the independent variables $\vec{x}_j$, given the set of parameters $\vec{\alpha}_k$. Monte Carlo simulated data

is used to validate the assumption that the fit variables are uncorrelated. The exponential factor in $\mathcal{L}$ accounts for Poisson fluctuations in the total number of observed events $N$. For the $K^{\pm}\pi^{\mp}$ terms the yields are rewritten in terms of the sum $n_f + n_{\bar{f}}$ and the asymmetry $\mathcal{A} = (n_{\bar{f}} - n_f)/(n_{\bar{f}} + n_f)$, where $n_f$ ($n_{\bar{f}}$) is the fitted number of events in the mode $B \to f$ ($\overline{B} \to \bar{f}$).

The parameters for both signal and background $m_{\rm ES}$, $\Delta E$, and $\mathcal{F}$ PDFs are determined from data, and are cross-checked with the parameters derived from Monte Carlo simulation. The $\theta_c$ PDFs are derived from kaon and pion tracks in the momentum range of interest from approximately 42 000 $D^{*+} \to D^0\pi^+$ ($D^0 \to K^-\pi^+$) decays. This control sample is used to parameterize the $\theta_c$ resolution as a function of track polar angle.

The results of the fit are summarized in Table 1. For the decay $B^0 \to K^+K^-$ we measure the branching fraction $\mathcal{B} = (0.85^{+0.81}_{-0.66} \pm 0.37) \times 10^{-6}$. The 90% confidence level upper limit for this mode is computed as the value $n_k^0$ for which $\int_0^{n_k^0} \mathcal{L}_{\rm max}\, dn_k / \int_0^{\infty} \mathcal{L}_{\rm max}\, dn_k = 0.90$, where $\mathcal{L}_{\rm max}$ is the likelihood as a function of $n_k$, maximized with respect to the remaining fit parameters. The result is then increased by the total systematic error. The reconstruction efficiency is reduced by its systematic uncertainty in calculating the branching fraction upper limit. The statistical significance of a given channel is determined by fixing the yield to zero, repeating the fit, and recording the square root of the change in $-2\ln\mathcal{L}$.

Table 1: Summary of results for reconstruction efficiencies ($\varepsilon$), fitted signal yields ($N_S$), statistical significances, and measured branching fractions ($\mathcal{B}$). The total number of events entering the ML fit is 16032. For the $K^+K^-$ mode the 90% confidence level (CL) upper limit for the branching fraction is quoted. Equal branching fractions for $\Upsilon(4S) \to B^0\overline{B}^0$ and $B^+B^-$ are assumed.

| Decay mode | $\varepsilon$ (%) | $N_S$ | Stat. Sig. ($\sigma$) | $\mathcal{B}(10^{-6})$ |
|---|---|---|---|---|
| $B^0 \to \pi^+\pi^-$ | 45 | $41 \pm 10 \pm 7$ | 4.7 | $4.1 \pm 1.0 \pm 0.7$ |
| $B^0 \to K^+\pi^-$ | 45 | $169 \pm 17 \pm 13$ | 15.8 | $16.7 \pm 1.6 \pm 1.3$ |
| $B^0 \to K^+K^-$ | 43 | $8.2^{+7.8}_{-6.4} \pm 3.5$ | 1.3 | $< 2.5$ |

Event-counting analyses, based on the same variable set $x_j$ as used in the fits, serve as cross-checks for the ML fit results. The variable ranges are generally chosen to be tighter in order to optimize the signal-to-background ratio, or upper limit, for the expected branching fractions. We count events in a rectangular signal region in the $\Delta E$–$m_{\rm ES}$ plane, and estimate the background from a sideband area. The branching fractions measured using this technique are in good agreement with those arising from the ML fit analysis. Figure 1 shows the distributions in $m_{\rm ES}$ for events passing the tighter selection criteria of the event-counting analyses.

The following sources of systematic uncertainty have been considered: imperfect knowledge of the PDF shapes, which translates into systematic uncertainties in both the fit yields and asymmetries; systematic uncertainties in the detection efficiencies, which affect only the branching ratio measurements; and possible charge biases in either track reconstruction or particle identification, which affect only the asymmetries.

The PDF shapes contribute the largest source of systematic uncertainty. Systematics due to uncertainties in the PDF parameterizations are estimated either by varying the PDF parameters within $1\sigma$ of their measured uncertainties or by substituting alternative PDFs from independent control samples, and recording the variations in the fit results. The largest systematic uncertain-

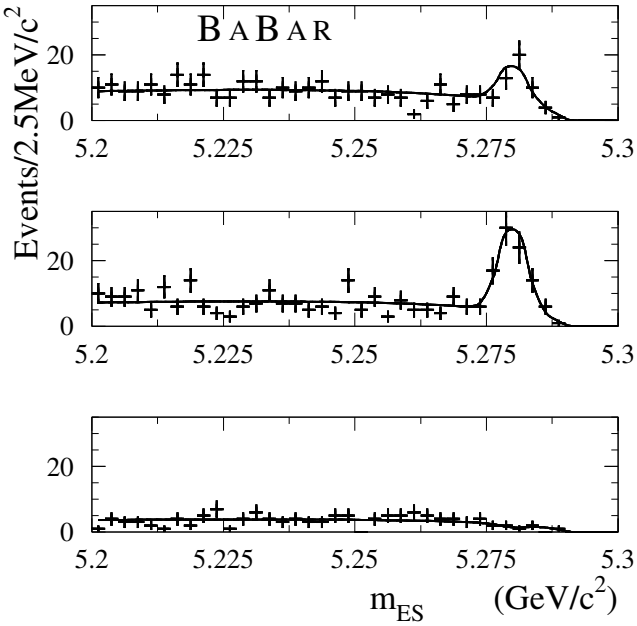


Figure 1: The $m_{\rm ES}$ distributions for candidates passing the selection criteria of the event-counting analyses for the $\pi^+\pi^-$ (top), $K^+\pi^-$ (center), and $K^+K^-$ (bottom) mode.

ties of this type vary across decay modes and are in the range 1%–7% . The total systematic uncertainties in the signal yields due to PDF systematics are given in Table 1.

The overall systematic uncertainties on the branching fractions as given in Table 1 are computed by adding in quadrature the PDF systematics and the systematic uncertainties on the efficiencies.

## 4 Non-resonant three-body modes and quasi-two-body modes

In Table 2 we summarize some earlier results that were obtained with a smaller datasample of 7.7 fb$^{-1}$ on-resonance, corresponding to 8.8 million $B\overline{B}$ pairs, and 1.2 fb$^{-1}$ off-resonance. For the details of these event-counting analyses we refer to Ref. 9.

Table 2: Summary of branching fraction measurements. Inequality denotes 90% CL upper limit, including systematic uncertainties.

| Decay mode | $\mathcal{B}(10^{-6})$ | Decay mode | $\mathcal{B}(10^{-6})$ |
|---|---|---|---|
| $B^+ \to \pi^+\pi^-\pi^+$ | $< 22$ | $B^+ \to \eta' K^+$ | $62 \pm 18 \pm 8$ |
| $B^+ \to \rho^0\pi^+$ | $< 39$ | $B^0 \to \eta' K^0$ | $< 112$ |
| $B^0 \to \rho^\mp\pi^\pm$ | $49 \pm 13^{+6}_{-5}$ | $B^+ \to \omega K^+/\pi^+$ | $< 24$ |
| $B^+ \to K^+\pi^-\pi^+$ | $< 54$ | $B^+ \to \omega K^0$ | $< 14$ |
| $B^+ \to \rho^0 K^+$ | $< 29$ | $B^+ \to K^{*0}\pi^+$ | $< 28$ |

## 5 Conclusion

In summary, we have measured branching fractions for the rare charmless decays $B^0 \to \pi^+\pi^-$, $B^0 \to K^+\pi^-$, $B^0 \to \rho^\mp\pi^\pm$, and $B^+ \to \eta' K^+$, and set upper limits on $B^+ \to \pi^+\pi^-\pi^+$, $B^+ \to \rho^0\pi^+$, $B^+ \to K^+\pi^-\pi^+$, $B^+ \to \rho^0 K^+$, $B^0 \to \eta' K^0$, $B^+ \to \omega K^+/\pi^+$, $B^+ \to \omega K^0$, and $B^+ \to K^{*0}\pi^+$. Our results are in good agreement with earlier measurements [10].

## Acknowledgments

We wish to thank our PEP-II colleagues for their outstanding efforts in providing us with excellent luminosity and machine conditions. This work is supported by the US Department of Energy and National Science Foundation, the Natural Sciences and Engineering Research Council (Canada), Institute of High Energy Physics (China), the Commissariat à l'Energie Atomique and Institut National de Physique Nucléaire et de Physique des Particules (France), the Bundesministerium für Bildung und Forschung (Germany), the Istituto Nazionale di Fisica Nucleare (Italy), the Research Council of Norway, the Ministry of Science and Technology of the Russian Federation, and the Particle Physics and Astronomy Research Council (United Kingdom).

## References

[1] N. Cabbibo, Phys. Rev. Lett. **10**, 531 (1963); M. Kobayashi and T. Maskawa, Prog. Theor. Phys. **49**, 652 (1973).

[2] T. Hara, these proceedings.

[3] D. Lange, these proceedings.

[4] M. Gronau and D. London, Phys. Rev. Lett. **65**, 3381 (1990); M. Gronau, J.L. Rosner and D. London, *ibid.* **73**, 21 (1994); R. Fleischer, Phys. Lett. B **365**, 399 (1996); R. Fleischer and T. Mannel, Phys. Rev. Lett. **57**, 2752 (1998); M. Neubert and J. Rosner, Phys. Lett. B **441**, 403 (1998); M. Neubert, J. High Energy Phys. **02**, 014 (1999); M. Neubert, Nucl. Phys. Proc. Suppl. **99**, 113 (2001).

[5] J. Panetta, these proceedings.

[6] G. C. Fox and S. Wolfram, Phys. Rev. Lett. **41**, 1581 (1978).

[7] S.L. Wu, Phys. Rep. **107**, 59 (1984).

[8] CLEO Collaboration, D.M. Asner *et al.,* Phys. Rev. D **53**, 1039 (1996).

[9] *BABAR* Collaboration, B. Aubert *et al., Measurements of charmless three-body and quasi-two-body B decays*, *BABAR*-CONF-00/15, submitted to the XXX$^{\text{th}}$ International Conference on High Energy Physics, Osaka, Japan.

[10] CLEO Collaboration, D. Cronin-Hennessy *et al.,* Phys. Rev. Lett. **85**, 515 (2000); CLEO Collaboration, S.J. Richichi *et al., ibid.* **85**, 520 (2000); CLEO Collaboration, C.P. Jessop *et al., ibid.* **85**, 2881 (2000).